Biochemistry. Author manuscript; available in PMC 2016 August 31.

Published in final edited form as:
Biochemistry. 2010 October 26; 49(42): 9046–9057. doi:10.1021/bi1011496.

Inscribing the Perimeter of the PagP Hydrocarbon Ruler by Site-Specific Chemical Alkylation†

M. Adil Khan[‡], **Joel Moktar**[‡], **Patrick J. Mott**[‡], **Mary Vu**[‡], **Aaron H. McKie**[§], **Thomas Pinter**[§], **Fraser Hof**[§], and **Russell E. Bishop**[‡,*]

[‡]Department of Biochemistry and Biomedical Sciences and Michael G. DeGroote Institute for Infectious Disease Research, McMaster University, Hamilton, ON, Canada L8N 3Z5

[§]Department of Chemistry, University of Victoria, Victoria, BC, Canada V8W 3 V6

Abstract

The *Escherichia coli* outer membrane phospholipid:lipid A palmitoyltransferase PagP selects palmitate chains using its β-barrel-interior hydrocarbon ruler and interrogates phospholipid donors by gating them laterally through an aperture known as the crenel. Lipid A palmitoylation provides antimicrobial peptide resistance and modulates inflammation signaled through the host TLR4/MD2 pathway. Gly88 substitutions can raise the PagP hydrocarbon ruler floor to correspondingly shorten the selected acyl chain. To explore the limits of hydrocarbon ruler acyl chain selectivity, we have modified the single Gly88Cys sulfhydryl group with linear alkyl units and identified C10 as the shortest acyl chain to be efficiently utilized. Gly88Cys-*S*-ethyl, *S*-*n*-propyl, and *S*-*n*-butyl PagP were all highly specific for C12, C11, and C10 acyl chains, respectively, and longer aliphatic or aminoalkyl substitutions could not extend acyl chain selectivity any further. The donor chain length limit of C10 coincides with the phosphatidylcholine transition from displaying bilayer to micellar properties in water, but the detergent inhibitor lauryldimethylamine *N*-oxide also gradually became ineffective in a micellar assay as the selected acyl chains were shortened to C10. The Gly88Cys-*S*-ethyl and norleucine substitutions exhibited superior C12 acyl chain specificity compared to that of Gly88Met PagP, thus revealing detection by the hydrocarbon ruler of the Met side chain tolerance for terminal methyl group gauche conformers. Although norleucine substitution was benign, selenomethionine substitution at Met72 was highly destabilizing to PagP. Within the hydrophobic and van der Waals-contacted environment of the PagP hydrocarbon ruler, side chain flexibility, combined with localized thioetheraromatic dispersion attraction, likely influences the specificity of acyl chain selection.

PagP is an outermembrane palmitoyltransferase that catalyzes the transfer of a palmitate chain (16:0) fromthe *sn*-1 position of a glycerophospholipid to the free hydroxyl group of the (*R*)-3-hydroxymyristate chain at position 2 of lipid A (endotoxin) (Figure 1A) (1–3). In

†This work was supported by CIHR Operating Grant MOP-84329 awarded to R.E.B. and an NSERC Discovery Grant awarded to F.H. A. H.M. is a Pacific Century Scholar, and F.H. is a Career Scholar of the Michael Smith Foundation for Health Research and a CIHR New Investigator.

*To whom correspondence should be addressed: Department of Biochemistry and Biomedical Sciences, McMaster University, Health Sciences Centre 4H19, 1200 Main St. W., Hamilton, ON, Canada L8N 3Z5. Telephone: (905) 525-9140, ext. 28810. Fax: (905) 522-9033. bishopr@mcmaster.ca.

Escherichia coli and related pathogenic Gram-negative bacteria, PagP evades host immune defenses by resisting antimicrobial peptides (4–7) and attenuating the inflammatory response to infection triggered by lipopolysaccharide through the TLR4/MD2 pathway (8–10). Transcription of the *pagP* gene is governed by the PhoP/PhoQ regulon, which controls expression of bacterial lipid A modification enzymes induced during infection by host antimicrobial peptides (11, 12). PagP is thus a target for the development of anti-infective agents and a tool for the synthesis of novel vaccine adjuvants and endotoxin antagonists (2, 3).

The structure of *E. coli* PagP has been determined both by solution nuclear magnetic resonance spectroscopy and by X-ray crystallography, revealing an eight-strand antiparallel β-barrel preceded by an N-terminal amphipathic α-helix (13–15). Like other β-barrelmembrane proteins, the center of the PagP β-barrel is relatively rigid with more flexible external loops where the active site residues are localized. Although the catalytic mechanism remains to be elucidated, PagP alternates between two dynamically distinct states likely representing latent and active conformations in the outer membrane environment (16). PagP activity is triggered by outer membrane lipid asymmetry perturbations that enable the phospholipid and lipid A substrates to each have access to the active site from the external leaflet (17–19). Phospholipid and lipid A access occurs by lateral diffusion through two gateways in the β-barrel wall known as the crenel and embrasure, respectively (20) (Figure 1A). A 1.9Å resolution X-ray study of PagP inhibited by the detergent lauryldimethylamine *N*-oxide (LDAO)[1] revealed a buried LDAO molecule within the rigid β-barrel core, a site corresponding with the palmitoyl group binding pocket known as the hydrocarbon ruler (Figure 1A,B) (15). Recently, a 1.4 Å resolution X-ray structure of PagP crystallized from a mixture of sodium dodecyl sulfate (SDS) and 2-methyl-2,4-pentanediol (MPD) has revealed a crenel gating mechanism for the transit of the phospholipid between the hydrocarbon ruler and the outer membrane external leaflet (13).

PagP is exquisitely selective for a 16-carbon palmitate chain because its hydrocarbon ruler excludes lipid acyl chains differing in length by a solitary methylene unit (15, 21). Mutation ofGly88 lining the hydrocarbon ruler floor can modulate lipid acyl chain selection (21). Appropriate amino acid substitutions shorten the selected acyl chain by a degree predictable from the expected rise in the hydrocarbon ruler floor. In prior investigations of PagP hydrocarbon rulermutants, where Gly88Ala, Gly88Cys-*S*-methyl, and Gly88Met were constructed, acyl chain selection was predictably shifted toward C15, C13, and C12 acyl chains, respectively, with the expected unitary methylene resolution (21). These mutants display an aromatic exciton couplet during far-ultraviolet circular dichroism (far-UV CD) and a thermal unfolding temperature (T_u) of 88 °C that is characteristic of wild-type PagP (21). In this LDAO detergent system, PagP precipitates when unfolded above 80 °C(21). The

[1]Abbreviations: βME, β-mercaptoethanol; CD, circular dichroism; Kdo, 3-deoxy-D-*manno*-oct-2-ulosonic acid; DDM, *n*-dodecyl β-D-maltoside; ESI-MS, electrospray ionization mass spectrometry; EDTA, ethylenediaminetetraacetic acid; Gdn-HCl, guanidine hydrochloride; IPTG, isopropyl β-D-thiogalactopyranoside; LDAO, lauryldimethylamine *N*-oxide; MNBS, methyl *p*-nitrobenzenesulfonate; MPD, 2-methyl-2,4-pentanediol; Nle, norleucine; PDB, Protein Data Bank; PtdCho, phosphatidylcholine; PtdEtn, phosphatidylethanolamine; PBS, phosphate-buffered saline; SeM, selenomethionine; SDS, sodium dodecyl sulfate; T_u, thermal unfolding temperature; TLC, thin layer chromatography; UV, ultraviolet.

thermal melting profiles are thus at equilibrium only when a perturbation shifts the transition to temperatures below 80 °C (22).

Interestingly, the Gly88Cys mutant behaves as a dedicated myristoyltransferase at pH7, but at pH8, a buried thiolate anion extinguishes the exciton and destabilizes the enzyme so it selects both C14 and C15 acyl chains. Gly88Ser and Gly88Thr PagP mutants were also found to behave as myristoyltransferases having good stability, but only the Gly88Cys mutant at pH 7 was highly selective for myristate both in vitro and in vivo (22). Introduction of charged and polar groups more distally within the hydrocarbon ruler does not extinguish the exciton, but these substitutions do destabilize the enzyme and compromise the resolution of acyl chain selection (22). Branched uncharged polar groups and unbranched charged groups each support substantial low-resolution enzymatic activity in PagP Gly88 mutants, but groups that are both charged and branched are by comparison enzymatically inactive. Hydrocarbon ruler mutants with optimal stability and acyl chain resolution have so far been obtained primarily with unbranched aliphatic Gly88 substitutions, but the full extent of the hydrocarbon ruler remains to be elucidated.

Despite the widespread importance of integral membrane enzymes of lipid metabolism in signal transduction and membrane biogenesis processes (23, 24), their molecular mechanisms for lipid substrate interrogation remain poorly understood because many such enzymes have proven recalcitrant toward extraction from the membrane environment by a functional detergent (25). In contrast, PagP is a heat-stable 161-amino acid β-barrel enzyme, which intrinsically lacks Cys residues, and can reversibly unfold and refold in a defined detergent micellar enzymatic assay system (21). Methyl *p*-nitrobenzenesulfonate (MNBS) was previously used for site-specific chemical methylation ofGly88Cys PagP, and the S-methylated enzyme maintained stability and methylene unit acyl chain resolution (21). We have now prepared customized alkylating reagents to fully explore PagP hydrocarbon ruler acyl chain selectivity (Figure 1B,C). Like a piston inscribing the perimeter of a cylinder, we have mapped out the occluded surface of the hydrocarbon ruler and, simultaneously, evinced the nature of localized physical forces at work in determining its specificity.

EXPERIMENTAL PROCEDURES

Protein Expression and Purification

Cells were grown in LB mediumat 37 °C with ampicillin at 100 μg/mL or tetracycline at 12.5 μg/mL as appropriate (26). The expression and purification of PagP and its mutant derivatives were performed as previously described (21). The procedure depends on isopropyl β-D-thiogalactopyranoside (IPTG) induction in *E. coli* BL21-(DE3) from the pETCrcAHΔS vector, which removes the native signal peptide and introduces a C-terminal hexahistidine tag (14). Protein samples precipitated from water prior to detergent folding were dissolved in a 50:50 solution of 1% formic acid and acetonitrile just prior to electrospray ionization mass spectrometry (ESI-MS). The sample concentration was maintained at 1 ng/μL and the sample injected directly onto a Waters/Micromass Q-TOF Ultima Global quadrupole time-of-flight mass spectrometer. The spectra were reconstructed using the MassLynx 4.0 MaxEnt 1 module. Folded proteins were concentrated through Ni^{2+} affinity chromatography and dialyzed against 10 mM Tris-HCl (pH 8.0) and 0.1% LDAO to

remove imidazole and β-mercaptoethanol (βME). All protein stock solutions were maintained at a concentration of 2 mg/mL determined using the Edelhoch method (27) or bicinchoninic acid assay (28). Purified PagP and its mutant derivatives all display masses accurately matching theoretical predictions (Table 1). Site-directed mutagenesis was performed as described previously (21) to create Met72Leu PagP using the primers M72L-F (5′-GGCATGGCCTGTATGCCCTGGCATTTAAGGACTCGTGG-3′) and M72L-R (5′-CCACGAGTCCTTAAATGCCAGGGCATACAGGCCATGCC-3′). Three-dimensional portraits of PagP or the hydrocarbon ruler were rendered with PyMol (29) using an energy-minimized coordinate file, as described previously (21), and PDB entries 1THQ (15) and 3GP6 (13).

Preparation of Alkyl 4-Nitrobenzenesulfonates

Alkyl 4-nitrobenzenesulfonates were prepared by adaptation of a published method (Figure 1C) (30). The representative procedure was used for *n*-pentyl 4-nitrobenzenesulfonate. Metallic sodium (0.19 g, 8.4mmol, freshly cut and washed with hexanes to remove mineral oil)was added to *n*-pentyl alcohol (5mL) and the mixture allowed to react until gas evolution ceased. The resulting solution of sodium *n*-pentoxide was added in a dropwise manner to a solution of 4-nitrobenzenesulfonyl chloride (2.0 g, 8.4 mmol) in diethyl ether (50 mL) and the mixture stirred at room temperature under a nitrogen atmosphere. After 3 h, the reaction mixture was added to H_2O (100 mL) and the product was extracted with $CHCl_3$ (2 × 100 mL). The combined organics were washed with water (50 mL), saturated aqueous$NaHCO_3$ (100 mL), and water (50 mL) again prior to being dried overNa_2SO_4. The solvent was removed on a rotary evaporator and the crude product purified by column chromatography (SiO_2, 20% EtOAc in hexanes) to yield the pure product as a yellow solid (1.65 g, 72% yield): mp 55–56 °C; ^{1}H NMR (300 MHz, $CDCl_3$) δ 8.41 (d, 2H, *J* = 8.8 Hz), 8.12 (d, 2H, *J* =8.8 Hz), 4.14 (t, 2H, *J*= 6.5 Hz), 1.69 (m, 2H), 1.30 (m, 4H), 0.87 (t, 3H, *J* = 6.5 Hz); ^{13}C NMR (75 MHz, $CDCl_3$) δ 140.5, 127.5, 122.8, 113.0, 70.4, 26.9, 25.7, 20.3, 12.1.

The more elaborate *n*-aminopentyl 4-nitrobenzenesulfonate (Figure 3A) was prepared in two steps. A mixture of Boc-protected 5-amino-*n*-pentan-1-ol (0.25 g, 1.2 mmol) and dry CH_2Cl_2 (3 mL) was placed under a nitrogen atmosphere at 0 °C, and a solution of 4-nitrobenzenesulfonyl chloride (0.32 g, 1.2 mmol) dissolved in dry CH_2Cl_2 (3 mL) was added dropwise via syringe over the course of 15 min. The mixture was stirred at 0 °C for 2 h and allowed to warm to ambient temperature for 24 h. The reaction was quenched and the mixture subsequently washed three times with 1MHCl (5mL) and once with saturated aqueous NaCl (5 mL). The organic layer was dried over$MgSO_4$, filtered, and concentrated in vacuo. The crude yellow solid was dissolved in minimal EtOAc and purified by flash chromatography (SiO_2, 20 to 40% EtOAc in hexanes) to afford the corresponding Boc-protected 4-nitrobenzenesulfonate derivative as a pale yellow solid (0.28 g, 60% yield): mp 82–88 °C; ^{1}H NMR (300MHz, $CDCl_3$) δ 8.38 (d, 2H, *J*=9.1 Hz), 8.08 (d, 2H, *J*= 9.1 Hz), 4.49 (s, 1H), 4.11 (t, 2H, *J* = 6.5 Hz), 3.05 (q, 2H, *J* = 6.6 Hz), 1.65 (quintet, 2H, *J*=6.6 Hz), 1.48–1.30 (m, 13H); ^{13}C NMR (75MHz, $CDCl_3$) δ 156.1, 150.9, 142.1, 129.3, 124.6, 79.4, 71.7, 40.3, 29.6, 28.7, 28.5, 22.1; HRMS *m*/*z* 411.1201 [(M + Na)$^+$ calcd 411.1194]. A solution of this Boc-protected intermediate (0.05 g, 0.12 mmol) in MeOH (10 mL) was treated with HCl (1mL of a 4Msolution in dioxane). The mixture was stirred at ambient

temperature for 1 h, and all solvents were evaporated in vacuo. The crude yellow product was triturated in CH_2Cl_2, filtered, and washed with CH_2Cl_2 to afford the *n*-aminopentyl 4-nitrobenzenesulfonate product (Figure 3A) as its HCl salt (pale yellow solid, 0.024 g, 60% yield): mp 104–108 °C; ^{1}H NMR (500MHz, CD_3OD) δ 8.48 (d, 2H, J=8.8 Hz), 8.17 (d, 2H, J= 8.8 Hz), 4.19 (t, 2H, J = 6.2 Hz), 2.90 (t, 2H, J = 7.6 Hz), 1.75 (quintet, 2H, J = 7.6 Hz), 1.65 (quintet, 2H, J = 7.6 Hz), 1.46 (quintet, 2H, J = 7.5 Hz); ^{13}C NMR (125 MHz, CD_3OD) δ 151.2, 141.7, 129.3, 124.5, 71.1, 39.3, 28.3, 26.7, 25.3; HRMS m/z 289.0858 [$(M + H - Cl)^+$ calcd 289.0863].

Site-Specific Chemical Alkylation of Gly88Cys PagP

MNBS is commercially available, and we have previously adapted the S-methylation procedure developed by Heinrickson (31) for the covalent modification of Gly88Cys PagP (21). In the work presented here, the customized alkylating reagents described above were utilized to incorporate ethyl, *n*-propyl, *n*-butyl, *n*-pentyl, *n*-hexyl, and *n*-aminopentyl groups into the Gly88Cys PagPmutant. The reactions were conducted in capped glass tubes. To achieve buffer concentrations of 6 M guanidine hydrochloride (Gdn-HCl), 0.25 M Tris-HCl (pH 8.6), 3.3 mM disodium ethylenediaminetetraacetic acid (EDTA), and 25% acetonitrile (v/v), 25 mg of Gly88Cys PagP was dissolved in a volume of 3.75 mL of 8MGdn-HCl, 0.34MTris-HCl (pH 8.6), and 4.4 mM EDTA and the volume adjusted to 5 mL with 1.25 mL of 100%acetonitrile. The solutions were flushed with N_2 for 1min to create an anoxic barrier, and 50 μL of 260mMβMEwas added (10–50-fold molar excess of the protein). The tubes were tightly sealed and placed in a 50 °C bath for 1.5 h and then gradually cooled to 37 °C. Under aN_2 barrier, 0.5mL of 5.2mM ethyl, *n*-propyl, *n*-butyl, *n*-pentyl, *n*-hexyl, or *n*-aminopentyl 4-nitrobenzenesulfonate (2-fold molar excess of the βME) dissolved in acetonitrile was added to the reaction mixture. The reactions were conducted at 37 °C for 2 h with ethyl, 4 h with *n*-propyl, 8 h with *n*-butyl, and overnight with *n*-pentyl, *n*-hexyl, and *n*-aminopentyl 4-nitrobenzenesulfonate. Reactions were quenched by addition of 5 μL of 14 M βME. The reaction mixture was dialyzed exhaustively against distilled water, and the precipitated proteins were collected. A small amount of the precipitate was stored for the purposes of ESI-MS as described above. The remainder was dissolved in 10mMTris-HCl (pH8.0) and 6 M Gdn-HCl for protein refolding as described previously (21).

Norleucine and Selenomethionine Substitution

To incorporate norleucine (Nle) or selenomethionine (SeM) into PagP and its mutants, the appropriate expression plasmids were transformed into methionine auxotrophic cell line *E. coli* B834-(DE3). Nle incorporation was based on the procedure described by Budisa (32), except that we adapted media designed for SeM labeling. Four stock solutions were prepared. First, a stock solution of 50× amino acid mix was prepared by adding to 500 mL of autoclaved water 1 g each of the standard L-amino acids, excluding cystine, *trans*-proline, tyrosine, glutamine, and methionine. The solution was passed through a 0.22 μm filter, and 40mL aliquots were stored at −80 °C. Second, a 1000× trace metal stock solution was prepared to yield a final concentration in culture media of 10 μM for each metal: 12.4 g of $(NH_4)_6(Mo_7)_{24} \cdot 4H_2O$, 2.4 g of $CoCl_2 \cdot 6H_2O$, 2.5 g of $CuSO_4 \cdot 5H_2O$, 0.62 g ofH_3BO_3, 2.0 g of$MnCl_2 \cdot 4H_2O$, and 1.4 g of $ZnCl_2$ were added to 0.1% HCl in a final volume of 1.0 L and autoclaved. Third, a buffer solution was prepared by dissolving 4.0 g of $(NH_4)_2SO_4$,

18.0 g of KH_2PO_4, 42.0 g of K_2HPO_4, and 2.0 g of Na_3-citrate in 800 mL of water and autoclaved. Finally, we prepared the TyB "Tyrosine and nucleotide bases" mix by dissolving 0.16 g of tyrosine and 2.0 g each of adenine, guanosine, thymine, and uracil in 2.0 L of autoclaved water by heating the sample to 50 °C with stirring and then autoclaving. After the samples had been cooled to room temperature, the following were added to the TyBmix in order: 80mLof the 50°amino acid stock, 8 mL of 20 mg/mL glutamine (filter-sterilized), 80 mL of 50% glycerol (autoclaved), 5 mL of the 1000× trace metal mix, 4 mL of 0.5 M $CaCl_2$ (filter-sterilized), 4 mL of $MgSO_4$ (filter-sterilized), 1.6 mL of 5 mg/mL thiamine (filter-sterilized), 1000 mL of autoclaved water, and 800 mL of the buffer solution. The TyB mix was stored at 4 °C until it was used. A solution of Nle was also prepared via addition of 0.33 g to 10 mL of water for a final medium concentration of 5 mMat pH 2.31 and filter-sterilized.

For Nle substitution, wild-type, Gly88Met, and Gly88Cys PagP strains were grown in 5 mL of LB medium at 37 °C overnight, and 1 mL of each overnight culture was inoculated into 1 L of prewarmed minimal medium described above to which a limited amount of Met (0.05mM) had been added. After the OD reached 0.6, the Met-exhausted culture was supplemented with 5 mM Nle and incubated for 10 min before induction with 1mMIPTG. Cells were induced for 4 h at 37 °C before being harvested. As a control, we also grew these mutants in the same medium supplemented with 5mMMet. The protein was purified as described previously (21).

For SeM substitution, 10 mL overnight cultures of wild-type andGly88Met PagP strains were prepared in minimal medium as described above, but supplemented with 0.3mMMet. After 16 h, the cultures were harvested at 7000 rpm for 10min. The pellet was washed twice with 10 mL of minimal medium without Met and then resuspended in 20 mL of minimal medium supplemented with 0.05 mM Met. The suspension was then added to 980 mL of minimal medium supplemented with 0.05 mM Met. After an OD of 0.7 had been reached, 10 mL of a 300mMfilter-sterilized SeM solution was added to the Met-depleted culture to give a final SeM concentration of 3 mM. After incubation for 10 min, the culture was induced with 1 mM filter-sterilized IPTG and grown for 4 h before the cells were harvested. The protein was purified as described previously (21), except that solutions were maintained in a reduced state by addition of 20 mM βME. No oxidation of SeM to SeM selenoxide in PagP was evident by ESI-MS (Table 1).

CD Spectroscopy

Samples to be analyzed by far-UV CD were maintained at a concentration of 15 μM in 10mMTris-HCl (pH 8.0) and 0.1% LDAO using a cuvette with a path length of 1 mm. An Aviv 215 spectrophotometer was linked to a Merlin Series M25 Peltier device for temperature control. For each sample, three accumulations were averaged at a data pitch of 1 nm and a scanning speed of 10 nm/min. The temperature was maintained at 25 °C, and data sets were obtained from 200 to 260 nm for far-UV CD. Thermal denaturation profiles were obtained by heating the samples from20 to 100 °Cat 218 nm with a temperature slope of 2 °C/min and a response time of 16 s.

Preparation of [^{32}P]Kdo$_2$-Lipid A

To prepare radio labeled lipid A bearing two units of 3-deoxy-D-*manno*-oct-2-ulosonic acid (Kdo$_2$-lipid A), a 10 mL culture of *E. coli* WBB06 was grown overnight as described previously (33). Briefly, a 1:100 dilution was made in 5 mL of LB containing 25 μCi of [^{32}P]orthophosphate (Perkin-Elmer) and grown at 37 °C for 4–5 h. After being harvested, the pellet was washed with phosphate-buffered saline (PBS) (pH 7.4) (26) and harvested again. The cells were suspended in a $CHCl_3$/MeOH/PBS (pH 7.4) mixture (1:2:0.8, v/v) and allowed to sit at room temperature for 1 h with slight agitation. The tube was centrifuged at 7000 rpm and room temperature for 10 min, and the supernatant was collected. Appropriate amounts of $CHCl_3$ and H_2O were added to form a two-phase Bligh–Dyer solution [$CHCl_3$/MeOH/H_2O mixture (2:2:1.8, v/v)] (34), and the lower phase was extracted. The lower phase was dried under N_2, and the dried lipids were resuspended in a $CHCl_3$/MeOH/H_2O mixture (2:3:1, v/v) (solvent A) and applied to a DE-52 cellulose column. We prepared the resin by washing dryDE-52 resin with 2.4MNH_4-acetate three times and then washing the resin with distilled water. The resin was then washed twice with aMeOH/2.4MNH_4-acetatemixture (8:2, v/v) and then twice with a $CHCl_3$/MeOH/2.4MNH_4-acetatemixture (2:3:1, v/v). The resin was washed several times with solvent A to remove all the salt. This resin was packed in a glass column to which the sample was applied. The column was washed with 2 column volumes of solvent A and then eluted with serial 5–8 column volumes of solvent A containing 60, 120, 240, 360, and 480mMNH_4-acetate as the aqueous component. Ten microliters of each fraction was visualized by thin layer chromatography (TLC) in the $CHCl_3$/pyridine/88% formic acid/H_2O solvent system (50:50:16:5, v/v) to identify the fractions containing Kdo$_2$-lipid A with a monophosphate moiety at position 1. The TLC plates were visualized using a PhosphorImager (Molecular Dynamics).

Acyltransferase Assays

The hydrocarbon ruler assays were performed using a TLC-based approach as previously described (21). Synthetic *sn*-1,2-diacylphosphatidylcholine (PtdCho) with unbranched saturated acyl chains of defined composition, and Kdo$_2$-lipid A, were obtained from Avanti Polar Lipids (Alabaster, AL). The assays were conducted in 0.5 mL microcentrifuge tubes, in which sufficient Kdo$_2$-lipid A was added to achieve a concentration of 10 μM in a final assay volume of 25 μL. To this sample was added a trace amount of [^{32}P]Kdo$_2$-lipid A, yielding a density of 200 cpm/μL. Sufficient PtdCho was added to attain a final concentration of 1mM. These constituents were dried under a gentle N_2 stream and subsequently dissolved in 22.5 μL of a reaction cocktail containing 0.1 M Tris-HCl (pH 8.0), 10 mM EDTA, and 0.25% dodecyl maltoside (DDM). The reaction was initiated via addition of sufficient PagP, serially diluted in DDM to remove inhibitory LDAO, to achieve a linear reaction profile. All reactions were conducted at 30 °C and were stopped by directly spotting 4 μL of the reaction mixture to the origin of a Silica Gel 60 TLC plate. The TLC plate was resolved in a $CHCl_3$/pyridine/88% formic acid/H_2O system (50:50:16:5, v/v) within a tightly sealed glass tank. The constituents of the tank were allowed to equilibrate for a period of 3 h prior to being exposed to the TLC plate. After the plate was dried, it was exposed to a Molecular Dynamics PhosphorImager screen overnight to visualize the reaction. The product was quantified using ImageQuant. Detergent exchange acyltransferase assays for wild-type and Gly88Cys-*S*-*n*-butyl PagP were conducted by dilution of the protein samples

in reaction buffers containing either 0.25% DDM, 0.1% Cyclofos 7, or 0.1% LDAO [all detergents were obtained from Anatrace (Maumee, OH)]. Wild-type PagP was assayed using di16:0 PtdCho, and Gly88Cys-*S*-*n*-butyl PagP was assayed using di10:0 PtdCho. The inhibitory effects of LDAO upon PagP were determined via addition of increasing concentrations of LDAO to the assay.

RESULTS AND DISCUSSION

PagP and its mutants were produced in *E. coli* BL21(DE3) using IPTG-inducible PagP expression plasmid pETCrcAHΔS (14). The expressed proteins possess a C-terminal hexahistidine tag and lack the N-terminal signal peptide to target PagP for secretion to the outer membrane. The proteins are expressed as insoluble aggregates, which can be dissolved in Gdn-HCl, purified by Ni^{2+}-ion affinity chromatography, and folded by dilution into the detergent LDAO (21). Site-specific chemical alkylation of Gly88Cys PagP was performed by an established procedure (Figure 1B) (21, 31) and confirmed by ESI-MS of the purified proteins (Table 1). Alkyl *p*-nitrobenzenesulfonates were prepared from the corresponding sodium alkoxides and 4-nitrobenzenesulfonyl chloride as described in Experimental Procedures (Figure 1C). PagP phospholipid:lipid A palmitoyltransferase activity is monitored in vitro using a defined detergent micellar enzymatic assay with TLC separation of radioactive lipid products (21). The inhibitory LDAO detergent used during PagP folding is exchanged by dilution into DDM to support enzymatic activity. Wild-type PagP is highly selective for a palmitoyl group at the *sn*-1 position in a glycerophospholipid but largely unspecific for the polar headgroup (1). We employ the palmitoyl donor di-16:0-PtdCho and the palmitoyl acceptor [^{32}P]Kdo_2-lipid A. When challenged with a spectrum of donor acyl chain lengths, wild-type PagP functions as a dedicated palmitoyltransferase whereas Gly88 PagP mutants can utilize shorter acyl chains.

Analysis of Gly88Cys-S-alkyl Mutants

We examined the hydrocarbon ruler profiles for the Gly88Cys-*S*-alkyl PagP derivatives using a suite of diacyl PtdCho's varying in saturated acyl chain length fromC14 to C8 (Figure 2A). Gly88Cys-*S*-ethyl, *S*-*n*-propyl, and *S*-*n*-butyl PagP were all highly specific for C12, C11, andC10 acyl chains, respectively. As expected, Gly88Cys-*S*-*n*-pentyl PagP utilized a C9 acyl chain optimally, but with only half the specific activity compared to that of the wild type and the shorter alkyl substitutions when using their optimal substrates. Gly88Cys-*S*-*n*-hexyl PagP was by comparison inactive (Figure 2A). Far-UV CD analysis of the folded *S*-alkylated proteins clearly identified the positive 232 nm ellipticity derived from the intact aromatic exciton (Figure 2B) (21). The T_u of 88 °C for wild-type PagP β-barrel unfolding is elevated by ~2–4 °C among the spectrum of Gly88Cys-*S*-alkyl derivatives (Figure 2C). Additionally, the 218 nm component of the exciton is observed by its loss above 40 °C, consistent with the known thermal sensitivity of the exciton (Figure 2C) (21). We had previously observed an ~2 °C increase in thermal stability for Gly88Cys-*S*-methyl PagP (21), and that finding is recapitulated here (Figure 2C). Although S-alkylation appears to stabilize PagP by occluding the hydrocarbon ruler cavity (Figure 2C), such stabilization was not observed in Gly88Met PagP (21).

The observed donor chain length limit of C10 (Figure 2A) happens to coincide with the PtdCho transition from displaying bilayer to micellar properties in water (35). If shorter acyl chains had been supported, a substrate that also functioned as a detergent might have replaced DDM in the in vitro PagP assay system. DDM thus remains an intrinsic component of the assay, but its detergent properties disrupt bilayer phospholipid phase behavior (25). The C10 limit might better reflect the minimal occluded surface area between the donor acyl chain and hydrocarbon ruler required for PagP to selectively engage its substrate. We thus tested inhibition by the detergent LDAO, which also gradually became ineffective in the DDM micellar assay as the selected acyl chains were shortened to C10 (Figure 2D). Inhibition at 10 mM LDAO corresponds to a mole fraction of two LDAO molecules to one DDM molecule. Although LDAO inhibition in the mixed micelles was gradually lost, we could not replace DDM to assay the Gly88Cys-*S*-*n*-butyl PagP derivative in LDAO alone (Figure 2E). Either the LDAO at a high mole fraction can still inhibit competitively, or else the physical properties of the LDAO micelles themselves are somehow incompatible withGly88Cys-*S*-*n*-butyl PagP activity. The hydrocarbon ruler floor was shown previously to be solvent accessible when DDM supported the palmitoyltransferase reaction, but solvent exchange and enzymatic activity were both blocked when the enzyme was folded in LDAO micelles (22). DDM and Cyclofos-7 remain the only detergents known to support PagP activity without interfering as unspecific substrates or as competitive inhibitors (15, 16).

Effect of Incorporation of Ammonium Ion within the Hydrocarbon Ruler

A recent 1.4Å resolution X-ray structure of PagP crystallized from SDS/MPD has revealed a single SDS detergent molecule buried within the hydrocarbon ruler (13). The nine terminal carbons of the SDS molecule are tightly held and take a zigzagging electron density pattern in contrast to the tubular pattern observed closer to the headgroup. In the terminal eight carbons of the acyl chain, the SDS in the pocket overlaps very well with the LDAO molecule at 1.9Å resolution (15), but the paths diverge closer to the headgroup region (Figure 3A). If the bound detergent molecules correspond to a palmitoyl group in the Michaelis complex, then the overlapping detergent electron density might define the fully occluded surface of the hydrocarbon ruler. Alternatively, the SDS molecule might better indicate the full hydrocarbon ruler because it extends further than the LDAO molecule before diverging. We have previously shown that Gly88Lys introduces a structural destabilization into PagP (T_u = 74 °C) that broadens the spectrum of selected acyl chains, but with the preferred substrate being the expected C11 (22). We wondered if providing an aminoalkyl substitution might extend acyl chain selection beyond the limit of C10 observed with our Gly88Cys-*S*-alkyl substitutions (Figure 2A). By incorporating an *n*-aminopentyl group using the corresponding aminoalkylating reagent (see Experimental Procedures), we tested for acyl chain selection out to C8 but found theGly88Cys-*S*-*n*-aminopentyl PagP to be enzymatically inactive by comparison with Gly88Lys PagP (Figure 3A). The incorporation of ammonium groups is most easily discerned by comparisons between two different pairs of nearly isosteric partners: Gly88Nle with Gly88Lys and Gly88Cys-*S*-*n*-hexyl with Gly88Cys-*S*-*n*-aminopentyl. Far-UV CD (Figure 3B) showed no major structural perturbation, while thermal melts (Figure 3C) showed that both NH^{3+}-containing partners were destabilized by the same amount relative to their CH_3-terminated counterparts. Unlike the significant differences observed between *S*-ethylcysteine and Met (see below), these data show no

dependence on the location of the ammonium ion in the folded state. This suggests that the large desolvation energy penalties that must be paid to bury an ammoniumion in the core of a protein are the dominant effects for this set of compounds.

Role of Side Chain Flexibility and Localized Thioether–Aromatic Dispersion Attraction in Engineering a Dedicated PagP Lauroyltransferase

TheC10 acyl chain transition most likely specifies diminishing binding forces between van der Waals-contacted groups localized within a hydrophobic microenvironment. In the absence of water or electrostatic perturbations, London dispersion forces appear to be a dominant source of intermolecular attraction, especially when nonpolar surface contacts are maximized without steric repulsion (36). Localized dispersive attractions should be paramount for the highly polarizable thioether sulfur atom, which is more electron-dense than typical hydrocarbon moieties (37). If a thioether-containing side chain fits snugly within the hydrocarbon ruler, van der Waals-contacted dispersive attractions with neighboring aromatic side chains should be more pertinent compared to interactions with aliphatic or hydroxylated side chains that lack conjugated resonance-stabilized π-electron systems (38, 39).

Interestingly, Gly88Cys-*S*-ethyl PagP behaves as a dedicated lauroyltransferase (Figure 2A), but acyl chain selection by its regioisomer Gly88Met PagP is imperfect by comparison (21) (Figure 4A). The main observed differences are the partial utilization of a C13 acyl chain byGly88Met PagP and the T_u that is increased from 88 °C, for wild-type and Gly88Met PagP, to 92 °C, for Gly88Cys-*S*-ethyl PagP (Figures 2C and 4B). To dissect the possible contribution of localized thioether–aromatic dispersion attraction from side chain conformational preferences, we substituted Met residues with the unnatural amino acid Nle through misaminoacylation of $tRNA^{Met}$ (32) (see Experimental Procedures). Substituting the five methionines in wild-type and Gly88Cys PagP (six in Gly88Met PagP) with Nle does not compromise structure and stability as ascertained by far-UV CD and thermal melts (Figure 4B,C). However, Nle substitution of Gly88Met PagP corrects the imperfect acyl chain selection, thus creating another dedicated lauroyltransferase, but without increasing its T_u (Figure 4A,C).

We interpret these findings in terms of the preferred conformational equilibria for the *n*-butyl side chain of Nle versus the thioether side chains of Met and *S*-ethylcysteine, combined with localized thioether–aromatic dispersion attraction solely for *S*-ethylcysteine. As cogently articulated by Gellman (36), the Nle side chain displays an enthalpic preference for the extended *anti* conformation, whereas Met slightly favors one of the two available *gauche* conformers (Figure 4D). We calculated identical gas-phase bond rotation barriers and conformational energies for the side chains of *S*-ethylcysteine and Met, indicating that differences in their acyl chain selectivity and thermal stability must be explained by interactions these side chains experience within the folded structure of PagP. Although the inherent conformational flexibility of Met is matched by that of *S*-ethylcysteine, only the latter substitution displays a stabilized T_u of 92 °C, which appears to lock the side chain in the extended *anti* conformation as is evident in its superb C12 acyl chain selectivity. Reflecting the thioether sulfur atom to the opposite wall of the hydrocarbon ruler in

Gly88Met PagP causes the local environment to support only the wild-type T_u of 88 °C. Without any corresponding stabilization, the Met thioether side chain is now free to explore its wider available conformational space and thus opens the hydrocarbon ruler for partial utilization of C13 acyl chains. The same reasoning can be applied to Gly88Cys-*S*-methyl PagP, which has the same terminal methyl group flexibility as Met, but is stabilized by an apparent thioetheraromatic dispersion attraction (T_u=90°C), thus locking the side chain in its extended conformation to yield superb selection of C13 acyl chains (21). This localized stabilization might also explain the excellent acyl chain selectivity of Gly88Cys-*S*-*n*-propyl and Gly88Cys-*S*-*n*-butyl PagP (Figure 2A,C). Gly88Met [Nle] PagP is a dedicated lauroyltransferase only because it intrinsically prefers the extended *anti* conformer, but without the thioether sulfur atom, it does not display the stabilized T_u (Figure 4C).

The hydrocarbon ruler microenvironments surrounding the bound detergent methylene groups, which correspond with the thioether sulfur atoms in Gly88Met PagP (position 14) or Gly88Cys-*S*-ethyl PagP (position 15), lend support to a role for localized thioether–aromatic dispersion attraction only for the latter substitution (Figure 5A). Whereas the thioether sulfur atom of Gly88Cys-*S*-ethyl PagP is likely cradled in its extended *anti* conformation at position 15 by the aromatic side chains of Tyr70, Trp156, and Tyr26, the same atom in Met at position 14 is likely exposed to the phenolic oxygen atom of Tyr70 together with the hydroxylated Thr108 and aliphatic Leu128. These distinctly different microenvironments might explain the observed stabilization of the same thioether sulfur atom only when it is localized at the deeper of the two hydrocarbon ruler positions (38, 39).

SeM Substitution Is Highly Destabilizing to PagP

To further explore the role of dispersion forces within the PagP hydrocarbon ruler, we replaced each Met residue (Figure 5B) with SeM, which introduces a larger and more electron dense selenium atom in place of sulfur. SeM is routinely used for phasing in X-ray crystallography, but its utility appears to be underrepresented among integral membrane protein structures (40). PagP [SeM] did not crystallize in our original structure determination, but mixing the labeled and native proteins did yield crystals suitable for phasing (15). Instability associated with SeM labeling of the β-barrel membrane protein FadL has also been reported (41). SeM-labeled wild-type and Gly88Met PagP were prepared in the presence of βME, and no oxidation of SeM to SeM selenoxide was evident by ESI-MS (Table 1). Although the exciton and β-barrel structure of PagP are evident in far-UV CD, we were surprised by the extent of the destabilization associated with SeM substitution in the corresponding thermal melts (Figure 6A,B). The greatest instability previously associated with an active PagP mutant is that of Gly88Cys PagP at pH 8, which loses its exciton and has its T_u reduced by 22 °C because of a buried thiolate anion (21) (see also Figure 4B,C). By comparison, SeM-substituted wild-type and Gly88Met PagP each display the exciton, but their T_u values are reduced by 34 °C (Figure 6B). PagP with Nle and PagP without Nle were virtually indistinguishable in terms of stability (Figure 4C), and wild-type acyl chain selection (Figure 6C) was not distinctly different for the Nle-substituted protein (not shown). However, SeM substitution of the five intrinsic Met residues drastically broadened acyl chain selection and reduced the specific activity (Figure 6C). The introduction of a sixth SeM residue at position 88 did not further destabilize the protein

(Figure 6B), but the residual enzymatic activity was extinguished (Figure 6D). We conclude that substituting Met88 with SeM compromises lipid acyl chain selection without any apparent PagP destabilization.

Of the five Met residues in wild-type PagP, only Met72 is buried and lines the hydrocarbon ruler wall (Figures 1B and 5). Two conformers of this thioether side chain are apparent in the SDS/MPD structure (13), and the corresponding selenide might be envisaged to influence lipid acyl chain selection from this position through disruption of neighboring van der Waals packing interactions (Figure 6C). We purified Met72Leu PagP, both with and without SeM substitution (Table 1), and found Met72 to be entirely responsible for the perturbation observed in the wild-type enzyme upon SeM substitution (Figure 7). No destabilization was associated with SeM substitution of the four surface-exposed SeM residues. Met6 and the non-nativeMet0 are each located in the N-terminal helix, whereas the C-terminal Met140 and Met157 are both exposed on the β-barrel surface (Figure 5B). These four surface residues all map onto the belt of high hydrophobic surface potential marking the transmembrane domain in the 1.4Å resolution SDS/MPD structure (13, 42). SeM residues buried within the hydrophobic core or exposed to solvent on the surface of soluble globular proteins are usually reasonably well tolerated (32, 40, 43). Our findings point to a strongly destabilizing influence of SeM at position 72 in PagP. The Lennard-Jones potential describes a narrow optimal distance range between neutral molecules for the ideal interaction energy to balance weak van der Waals attraction with stronger steric repulsion (44). We thus suspect that the larger van der Waals radius and/or bond lengths associated with the selenide compared to the sulfide at residue 72 are somehow incompatible with local packing arrangements necessary for optimal PagP stabilization (45).

Concluding Remarks

The thioether–aromatic dispersion attraction described here can also be regarded specifically as a methionine–π attraction (38), or more generally as a sulfide–π attraction (39). In an aqueous environment, the energetic stabilization of the methionine–π attraction is on the order of 0.3–0.5 kcal/mol (38). Similarly, conformational energies at equilibrium in the gas phase indicate that the Nle side chain enthalpically favors the *anti* conformer (Figure 4D) by 0.8 kcal/mol (36, 46). In our LDAO detergent system, these energetics translate into a T_u increase of 2–4 °C for the *S*-alkylated Gly88Cys PagP derivatives. Coulombic repulsions are typically stronger than London dispersion attractions (44), hence the 14 and 22 °C decreases in T_u observed with the buried ammonium (Figure 3C) (22) and thiolate ions (Figure 4C) (22), respectively. The observed destabilization attributed to SeM substitution ofMet72 is 34 °C, thus revealing the energetics of this steric repulsion to be stronger than the electrostatic perturbations.

The conclusion that the thioether bond cannot be regarded as simply equivalent to its corresponding methylene unit was made previously in a study using aminoalkylbromides to modify an introduced Cys residue in RNase A (47). Iodoalkanes have also been reported previously to modify an introduced Cys residue in an investigation of protease inhibition (48). The outer membrane phospholipase OMPLA was more recently subjected to covalent modification of its nucleophilic Ser residue using a suite of alkylsulfonylfluorides, thus

demonstrating alkyl chain length is the primary factor controlling its monomer–dimer equilibrium (49, 50). Our use of alkylnitrobenzenesulfonates to inscribe the PagP hydrocarbon ruler perimeter has allowed us to titrate the substrate affinity to the point where PagP can no longer function, all without changing the fold of the protein or dramatically altering the dispersion attractions governing lipid binding.

Acknowledgments

We thank Philip Hultin (University of Manitoba, Winnipeg, MB), Jian Payandeh (University of Washington, Seattle, WA), Alan Davidson (University of Toronto, Toronto, ON), and Murray Junop, Alba Guarné, Ricky Cheng, and Richard Epand (McMaster University) for helpful advice and discussions.

References

1. Bishop RE, Gibbons HS, Guina T, Trent MS, Miller SI, Raetz CR. Transfer of palmitate from phospholipids to lipid A in outer membranes of gram-negative bacteria. EMBO J. 2000; 19:5071–5080. [PubMed: 11013210]
2. Bishop RE. The lipid A palmitoyltransferase PagP: Molecular mechanisms and role in bacterial pathogenesis. Mol Microbiol. 2005; 57:900–912. [PubMed: 16091033]
3. Raetz CR, Reynolds CM, Trent MS, Bishop RE. Lipid A modification systems in gram-negative bacteria. Annu Rev Biochem. 2007; 76:295–329. [PubMed: 17362200]
4. Guo L, Lim KB, Poduje CM, Daniel M, Gunn JS, Hackett M, Miller SI. Lipid A acylation and bacterial resistance against vertebrate antimicrobial peptides. Cell. 1998; 95:189–198. [PubMed: 9790526]
5. Preston A, Maxim E, Toland E, Pishko EJ, Harvill ET, Caroff M, Maskell DJ. *Bordetella bronchiseptica* PagP is a Bvg-regulated lipid A palmitoyl transferase that is required for persistent colonization of the mouse respiratory tract. Mol Microbiol. 2003; 48:725–736. [PubMed: 12694617]
6. Pilione MR, Pishko EJ, Preston A, Maskell DJ, Harvill ET. *pagP* is required for resistance to antibody-mediated complement lysis during *Bordetella bronchiseptica* respiratory infection. Infect Immun. 2004; 72:2837–2842. [PubMed: 15102794]
7. Robey M, O'Connell W, Cianciotto NP. Identification of *Legionella pneumophila rcp*, a pagP-like gene that confers resistance to cationic antimicrobial peptides and promotes intracellular infection. Infect Immun. 2001; 69:4276–4286. [PubMed: 11401964]
8. Muroi M, Ohnishi T, Tanamoto K. MD-2, a novel accessory molecule, is involved in species-specific actions of *Salmonella* lipid A. Infect Immun. 2002; 70:3546–3550. [PubMed: 12065494]
9. Tanamoto K, Azumi S. *Salmonella*-type heptaacylated lipid A is inactive and acts as an antagonist of lipopolysaccharide action on human line cells. J Immunol. 2000; 164:3149–3156. [PubMed: 10706705]
10. Kawasaki K, Ernst RK, Miller SI. 3-*O*-Deacylation of lipid A by PagL, a PhoP/PhoQ-regulated deacylase of *Salmonella typhimurium*, modulates signaling through toll-like receptor 4. J Biol Chem. 2004; 279:20044–20048. [PubMed: 15014080]
11. Bader MW, Sanowar S, Daley ME, Schneider AR, Cho U, Xu W, Klevit RE, Le Moual H, Miller SI. Recognition of antimicrobial peptides by a bacterial sensor kinase. Cell. 2005; 122:461–472. [PubMed: 16096064]
12. Murata T, Tseng W, Guina T, Miller SI, Nikaido H. PhoPQ-mediated regulation produces a more robust permeability barrier in the outer membrane of *Salmonella enterica* serovar *typhimurium*. J Bacteriol. 2007; 189:7213–7222. [PubMed: 17693506]
13. Cuesta-Seijo JA, Neale C, Khan MA, Moktar J, Tran CD, Bishop RE, Pomès R, Privé GG. PagP crystallized from SDS/cosolvent reveals the route for phospholipid access to the hydrocarbon ruler. Structure. 2010; 18:1210–1219. [PubMed: 20826347]

14. Hwang PM, Choy WY, Lo EI, Chen L, Forman-Kay JD, Raetz CR, Prive GG, Bishop RE, Kay LE. Solution structure and dynamics of the outer membrane enzyme PagP by NMR. Proc Natl Acad Sci USA. 2002; 99:13560–13565. [PubMed: 12357033]
15. Ahn VE, Lo EI, Engel CK, Chen L, Hwang PM, Kay LE, Bishop RE, Prive GG. A hydrocarbon ruler measures palmitate in the enzymatic acylation of endotoxin. EMBOJ. 2004; 23:2931–2941.
16. Hwang PM, Bishop RE, Kay LE. The integral membrane enzyme PagP alternates between two dynamically distinct states. Proc Natl Acad Sci USA. 2004; 101:9618–9623. [PubMed: 15210985]
17. Bishop RE. Structural biology of membrane-intrinsic β-barrel enzymes: Sentinels of the bacterial outer membrane. Biochim Biophys Acta. 2008; 1778:1881–1896. [PubMed: 17880914]
18. Jia W, Zoeiby AE, Petruzziello TN, Jayabalasingham B, Seyedirashti S, Bishop RE. Lipid trafficking controls endotoxin acylation in outer membranes of *Escherichia coli*. J Biol Chem. 2004; 279:44966–44975. [PubMed: 15319435]
19. Smith AE, Kim SH, Liu F, Jia W, Vinogradov E, Gyles CL, Bishop RE. PagP activation in the outer membrane triggers R3 core oligosaccharide truncation in the cytoplasm of *Escherichia coli* O157:H7. J Biol Chem. 2008; 283:4332–4343. [PubMed: 18070877]
20. Khan MA, Bishop RE. Molecular mechanism for lateral lipid diffusion between the outer membrane external leaflet and a β-barrel hydrocarbon ruler. Biochemistry. 2009; 48:9745–9756. [PubMed: 19769329]
21. Khan MA, Neale C, Michaux C, Pomes R, Prive GG, Woody RW, Bishop RE. Gauging a hydrocarbon ruler by an intrinsic exciton probe. Biochemistry. 2007; 46:4565–4579. [PubMed: 17375935]
22. Khan MA, Moktar J, Mott PJ, Bishop RE. A thiolate anion buried within the hydrocarbon ruler perturbs PagP lipid acyl chain selection. Biochemistry. 2010; 49:2368–2379. [PubMed: 20175558]
23. van Meer G. Cellular lipidomics. EMBO J. 2005; 24:3159–3165. [PubMed: 16138081]
24. Forneris F, Mattevi A. Enzymes without borders: Mobilizing substrates, delivering products. Science. 2008; 321:213–216. [PubMed: 18621661]
25. Popot JL. Amphipols, nanodiscs, and fluorinated surfactants: Three nonconventional approaches to studying membrane proteins in aqueous solutions. Annu Rev Biochem. 2010; 79:737–775. [PubMed: 20307193]
26. Sambrook, J., Fritsch, EF., Maniatis, T. Molecular cloning: A laboratory manual. 2. Cold Spring Harbor Laboratory Press; Plainview, NY: 1989.
27. Edelhoch H. Spectroscopic determination of tryptophan and tyrosine in proteins. Biochemistry. 1967; 6:1948–1954. [PubMed: 6049437]
28. Smith PK, Krohn RI, Hermanson GT, Mallia AK, Gartner FH, Provenzano MD, Fujimoto EK, Goeke NM, Olson BJ, Klenk DC. Measurement of protein using bicinchoninic acid. Anal Biochem. 1985; 150:76–85. [PubMed: 3843705]
29. DeLano, WL. The PyMOL molecular graphics system. DeLano Scientific; San Carlos, CA: 2002.
30. Morgan MS, Cretcher LH. A kinetic study of alkylation by ethyl arylsulfonates. J Am Chem Soc. 1948; 70:375–378.
31. Heinrikson RL. The selective *S*-methylation of sulfhydryl groups in proteins and peptides with methyl-*p*-nitrobenzenesulfonate. J Biol Chem. 1971; 246:4090–4096. [PubMed: 5105446]
32. Budisa N, Steipe B, Demange P, Eckerskorn C, Kellermann J, Huber R. High-level biosynthetic substitution of methionine in proteins by its analogs 2-aminohexanoic acid, selenomethionine, telluromethionine and ethionine in *Escherichia coli*. Eur J Biochem. 1995; 230:788–796. [PubMed: 7607253]
33. Kanipes MI, Lin S, Cotter RJ, Raetz CR. Ca^{2+}induced phosphoethanolamine transfer to the outer 3-deoxy-D-*manno*-octulosonic acid moiety of *Escherichia coli* lipopolysaccharide. A novel membrane enzyme dependent upon phosphatidylethanolamine. J Biol Chem. 2001; 276:1156–1163. [PubMed: 11042192]
34. Bligh EG, Dyer WJ. A rapid method of total lipid extraction and purification. Can J Biochem. 1959; 37:911–917. [PubMed: 13671378]
35. Hauser H. Short-chain phospholipids as detergents. Biochim Biophys Acta. 2000; 1508:164–181. [PubMed: 11090824]

36. Gellman SH. On the role of methionine residues in the sequence-independent recognition of nonpolar protein surfaces. Biochemistry. 1991; 30:6633–6636. [PubMed: 2065050]
37. Fersht, A. Structure and mechanism in protein science:Aguide to enzyme catalysis and protein folding. 3. W. H. Freeman & Co; New York: 1998.
38. Tatko CD, Waters ML. Investigation of the nature of the methionine-π interaction in β-hairpin peptide model systems. Protein Sci. 2004; 13:2515–2522. [PubMed: 15322289]
39. Meyer EA, Castellano RK, Diederich F. Interactions with aromatic rings in chemical and biological recognition. Angew Chem, Int Ed. 2003; 42:1210–1250.
40. Morth JP, Sorensen TL, Nissen P. Membrane's Eleven: Heavy-atom derivatives of membrane-protein crystals. Acta Crystallogr. 2006; D62:877–882.
41. van den Berg B, Black PN, Clemons WM Jr, Rapoport TA. Crystal structure of the long-chain fatty acid transporter FadL. Science. 2004; 304:1506–1509. [PubMed: 15178802]
42. Evanics F, Hwang PM, Cheng Y, Kay LE, Prosser RS. Topology of an outer-membrane enzyme: Measuring oxygen and water contacts in solution NMR studies of PagP. J Am Chem Soc. 2006; 128:8256–8264. [PubMed: 16787090]
43. Yamniuk AP, Ishida H, Lippert D, Vogel HJ. Thermodynamic effects of noncoded and coded methionine substitutions in calmodulin. Biophys J. 2009; 96:1495–1507. [PubMed: 19217866]
44. Chang, R. Physical chemistry for the physical and biological sciences. University Science Books; Sausalito, CA: 2000.
45. Bondi A. van der Waals volumes and radii. J Phys Chem. 1964; 68:441–452.
46. Allinger NL, Yuh YH, Lii JH. Molecular Mechanics. TheMM3Force Field for Hydrocarbons 1. J Am Chem Soc. 1989; 111:8551–8566.
47. Messmore JM, Fuchs DN, Raines RT. Ribonuclease A: Revealing structure-function relationships with semisynthesis. J Am Chem Soc. 1995; 117:8057–8060. [PubMed: 21732653]
48. Hasan Z, Leatherbarrow RJ. A study of the specificity of barley chymotrypsin inhibitor 2 by cysteine engineering of the P1 residue. Biochim Biophys Acta. 1998; 1384:325–334. [PubMed: 9659394]
49. Stanley AM, Chuawong P, Hendrickson TL, Fleming KG. Energetics of outer membrane phospholipase A (OMPLA) dimerization. J Mol Biol. 2006; 358:120–131. [PubMed: 16497324]
50. Stanley AM, Treubrodt AM, Chuawong P, Hendrickson TL, Fleming KG. Lipid chain selectivity by outer membrane phospholipase A. J Mol Biol. 2007; 366:461–468. [PubMed: 17174333]

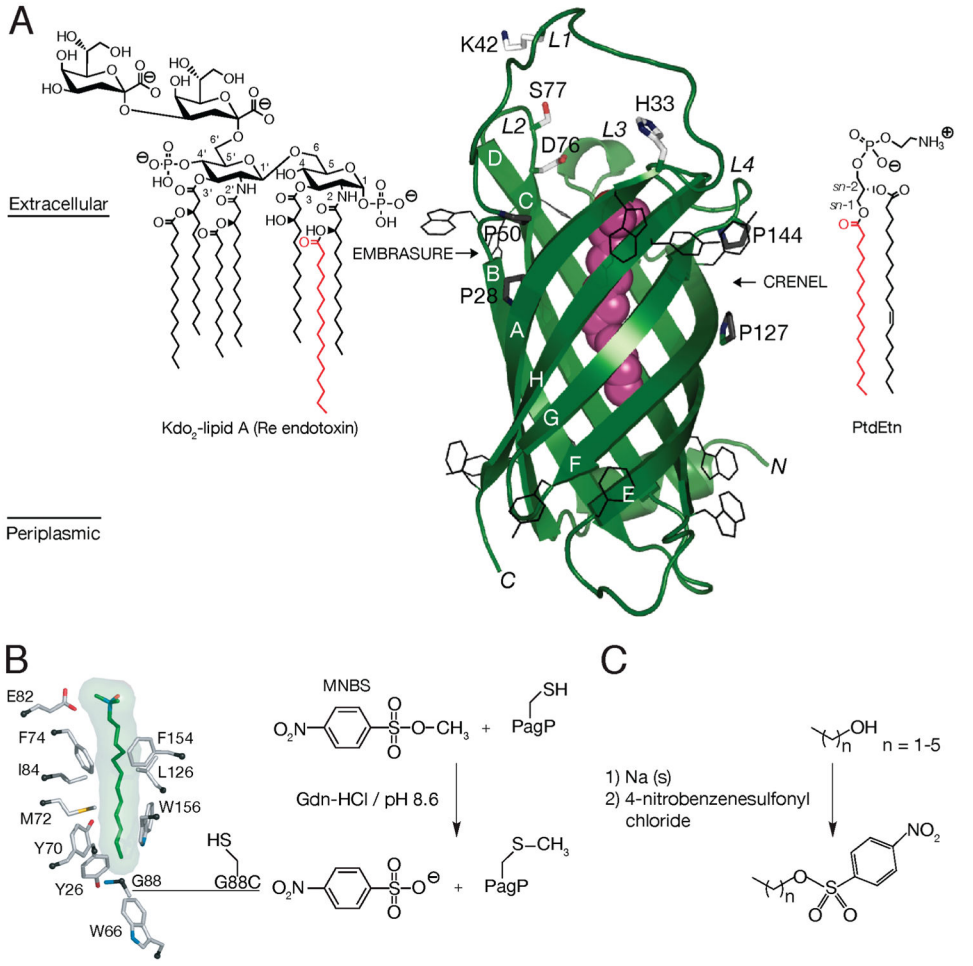

Figure 1.

Structural relationships among PagP, the hydrocarbon ruler, and *E. coli* outermembrane lipids. (A) *E. coli* PagP transfers a palmitoyl group (red) from the *sn*-1 position of a phospholipid, such as phosphatidylethanolamine (PtdEtn), to the free hydroxyl group of the N-linked (*R*)-3-hydroxymyristate chain at position 2 on the proximal glucosamine unit of lipid A. One of the simplest lipopolysaccharide acceptors for PagP in the outer membrane is known as Kdo_2-lipid A or Re endotoxin. PagP is an eight-strand antiparallel β-barrel preceded by an N-terminal amphipathic α-helix (colored green). The amino (N) and carboxyl (C) termini are labeled with black letters, and the β-strands are labeled with white letters (A–H). Aromatic belt residues (shown in wireframe format) demarcate the membrane interfaces between the extracellular and periplasmic spaces. A bound molecule of the detergent (colored magenta) delineates the interior hydrocarbon ruler. Points for lateral phospholipid access via the crenel (flanked by Pro127 and Pro144) and for lateral lipid A access via the embrasure (flanked by Pro28 and Pro50) are indicated. Although the catalytic mechanism is unknown, several key residues (shown in stick format) have been mapped to the extracellular surface loops (*L1–L4*). Loop L4 is disordered in the crystal structure (Protein Data Bank entry 1THQ) but has been introduced and energy minimized in the model shown. (B) A sagittal section reveals the bound LDAO molecule and residues

flanking the walls of the hydrocarbon ruler. A nondegenerate exciton interaction between Tyr26 and Trp66 manifests a couplet during far-UV CD spectroscopy. PagP far-UV CD exhibits positive exciton ellipticity at 232nm, and the negative ellipticity at 218 nm that arises more strongly from the β-barrel is also enhanced by the exciton. The adjacent Gly88 can be substituted to modulate lipid acyl chain selection. Gly88Cys functions as a dedicated myristoyltransferase at pH 7, but at pH 8, it introduces a destabilizing thiolate anion that extinguishes the exciton and broadens selection to include C15 acyl chains. Cys methylation with methyl *p*-nitrobenzenesulfonate (MNBS) restores the exciton at pH 8 and renders PagP selective for C13 acyl chains. (C) Synthetic scheme for a suite of alkyl *p*-nitrobenzenesulfonates used to inscribe the perimeter of the PagP hydrocarbon ruler by site-specific chemical alkylation.

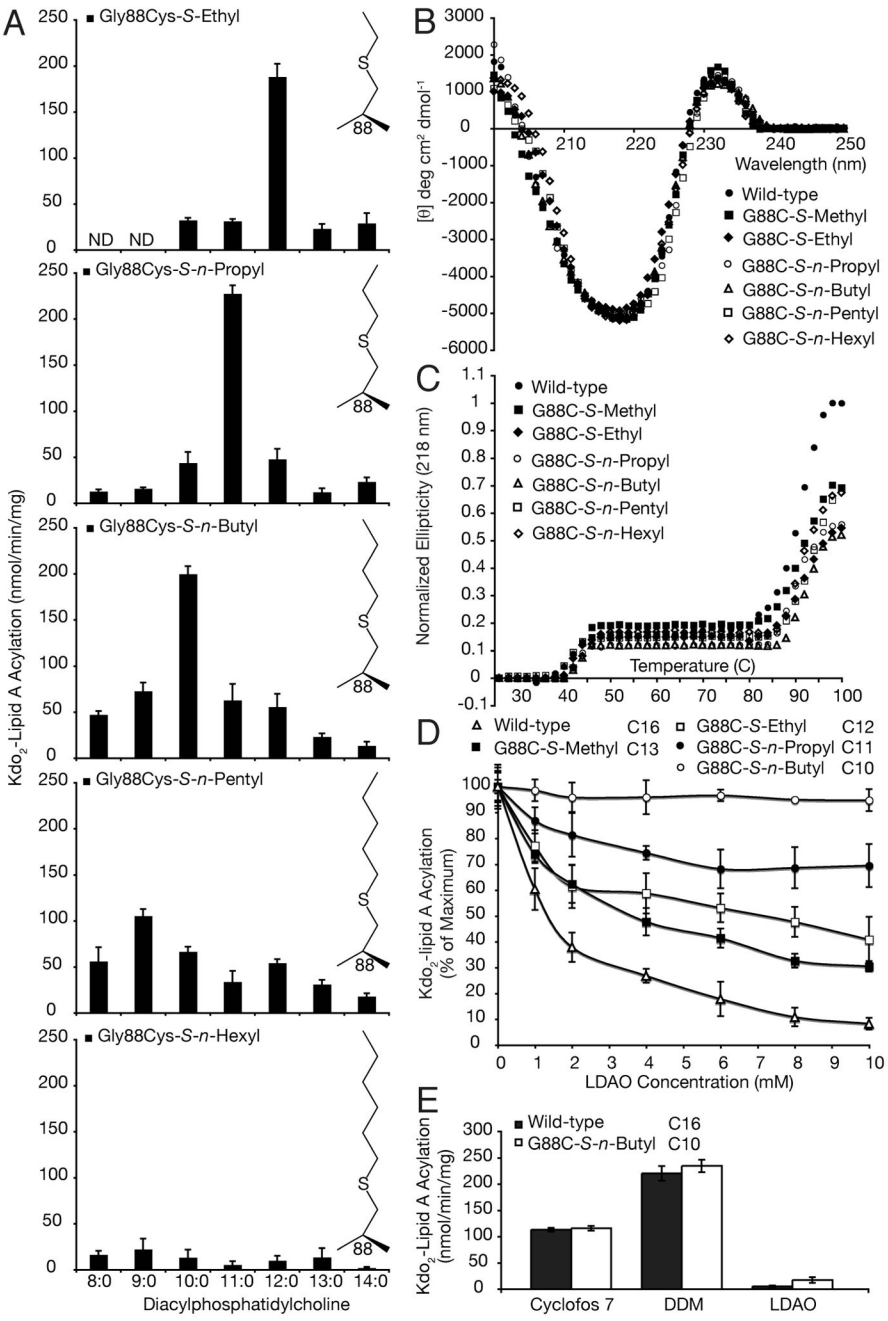

Figure 2.

Modulating the PagP hydrocarbon ruler by site-specific chemical alkylation. (A) PagP specific activity was monitored with a suite of PtdCho's having defined saturated acyl chain compositions varying from C14 to C8. Panels from top to bottom represent the activity profiles for Gly88Cys PagP modified with *S*-ethyl, *S*-*n*-propyl, *S*-*n*-butyl, *S*-*n*-pentyl, and *S*-*n*-hexyl alkyl groups, respectively. (B) Far-UV CD identifies the β-barrel and exciton signatures characteristic of wild-type PagP. (C) Thermal melts at 218 nm reveal exciton loss near 40 °C followed by β-barrel unfolding above 80 °C. (D) LDAO inhibition profiles for wild-type PagP and the Gly88Cys-*S*-alkyl substitutions using their preferred acyl chain

donors. (E) PagP specific activities for wild-type andGly88Cys-*S*-*n*-butyl PagP were assayed using C16 and C10 acyl chain donors, respectively, in three different detergent systems. ND means not detected.

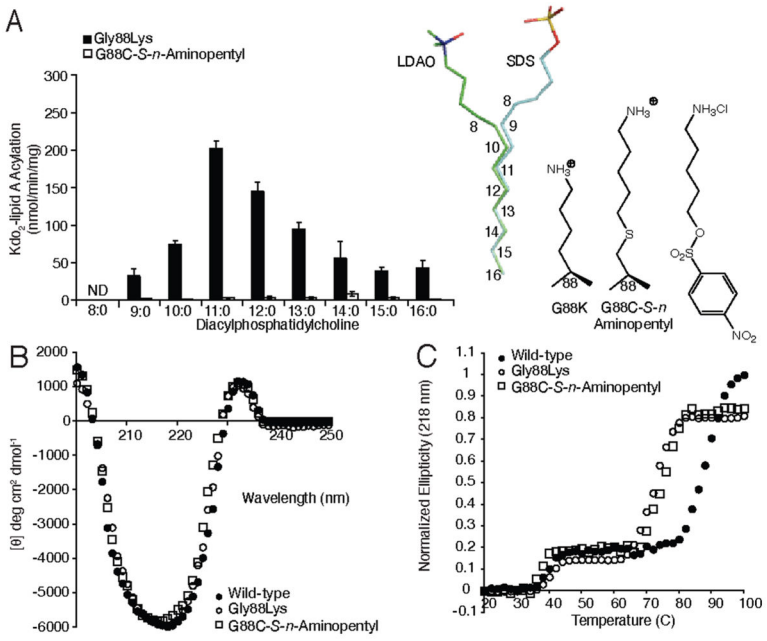

Figure 3.

Effect of the incorporation of ammonium ion within the hydrocarbon ruler. (A) PagP specific activity was measured using defined PtdCho's varying in saturated acyl chain length from C16 to C8 for the Gly88Lys and Gly88Cys-*S*-*n*-aminopentyl enzymes. Also shown is a superposition of bound LDAO and SDS molecules identified in the hydrocarbon ruler of two PagP crystal structures (PDB entries 1THQ and 3GP6). The numbering represents the positions that correspond to the carbon atoms of the palmitoyl group thought to occupy this position in the Michael is complex. The two detergents are aligned with the side chains of Gly88Lys and Gly88Cys-*S*-*n*-aminopentyl PagP together with the aminoalkylating reagent used to generate the latter substitution. Far-UV CD (B) and thermal melts at 218 nm (C) for wild-type PagP compared with those of Gly88Lys and Gly88Cys-*S*-*n*-aminopentyl PagP. ND means not detected.

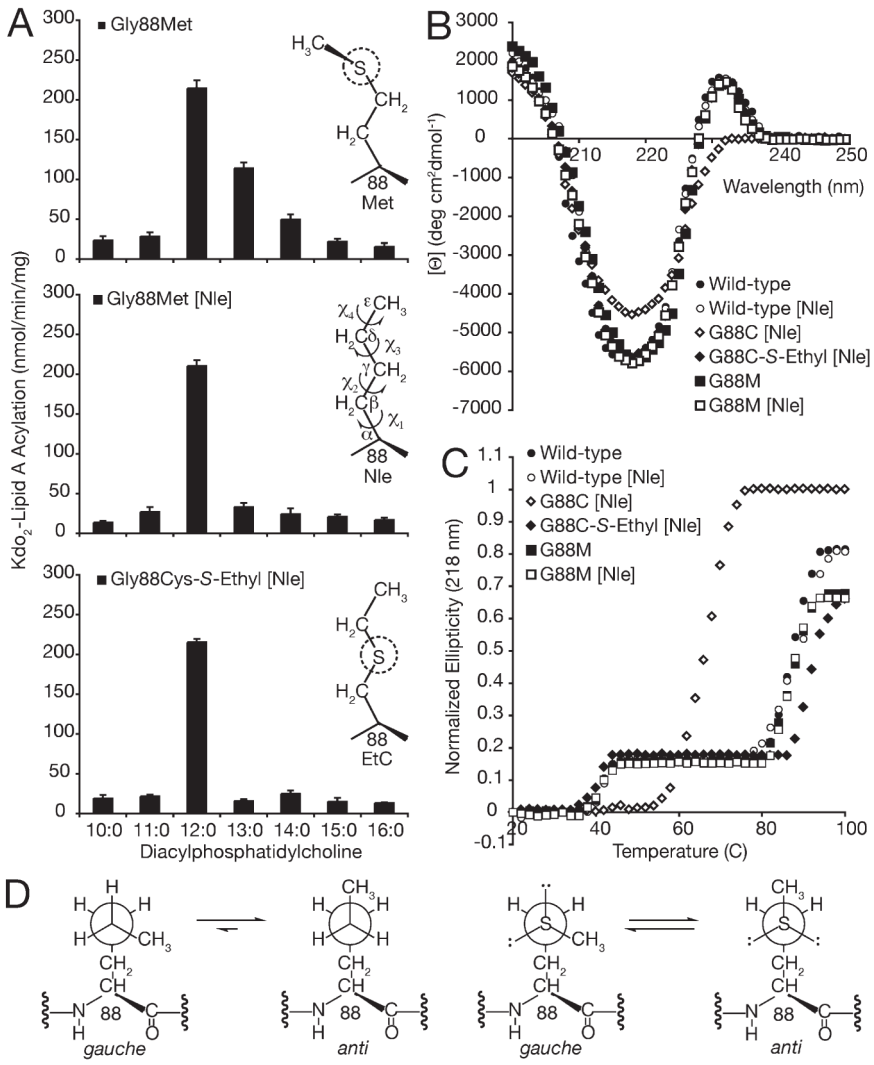

Figure 4.

Role of side chain flexibility and localized thioether–aromatic dispersion attraction in engineering a dedicated PagP lauroyltransferase. (A) PagP specific activity was measured using defined PtdCho's varying in saturated acyl chain length fromC16 toC10. The unnatural amino acid Nle was substituted for Met by misaminoacylation of $tRNA^{Met}$. Panels from top to bottom represent the activity profiles for Gly88Met, Gly88Met [Nle], and Gly88Cys-*S*-ethyl [Nle], respectively. For comparison, the behavior of Gly88Cys-*S*-ethyl PagP is shown in Figure 2. (B) Far-UVCD and (C) thermal melts at 218 nm reveal that substituting the five methionines in wild-type andGly88CysPagP (six inGly88MetPagP) with Nle does not compromise structure or stability. (D) Schematic representation of side chain conformational preferences for Nle (left) and Met (right). Viewed in Newman projection down the central χ^3 torsion axis, the penultimate atom is rotated to emphasize the enthalpic preference of Nle for maintaining the terminalmethyl group in the extended *anti* conformation, where as Met is slightly favored to adopt one of the two available *gauche* conformers.

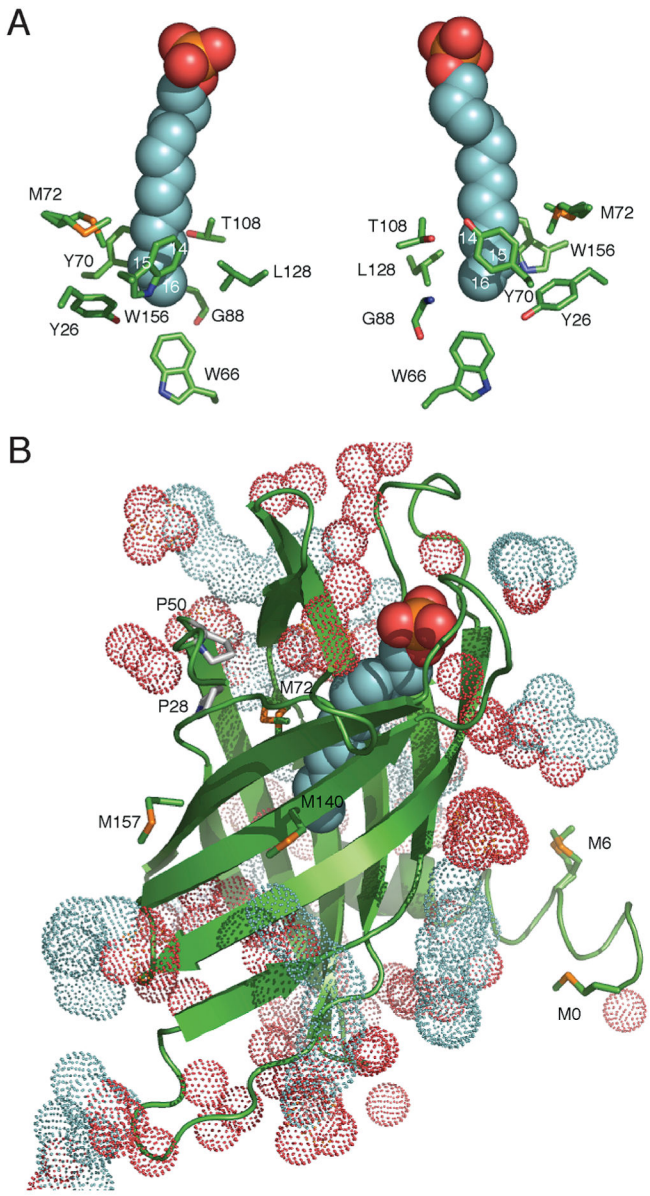

Figure 5.

Views of the hydrocarbon ruler and solvation shell for PagP in SDS/MPD. (A) Pseudo-2-fold symmetric views of the hydrocarbon ruler-bound SDS molecule (PDB entry 3GP6) emphasize the functional groups surrounding thioether positions 15 (Gly88Cys-*S*-alkyl) and 14 (Gly88Met), thus revealing distinctly different local environments for the sulfur atom. (B) Solvation of PagP in SDS/MPD at 1.4Å resolution reveals the belt of high hydrophobic surface potential. Met residues 0, 6, 72, 140, and 157 are shown as sticks, as are embrasure Pro residues 28 and 50. The buried SDS is shown in space-filling format, whereas the remaining 5 SDS, 56 water, 10 MPD, 6 sulfate, and 2 lithium molecules are shown in dots format.

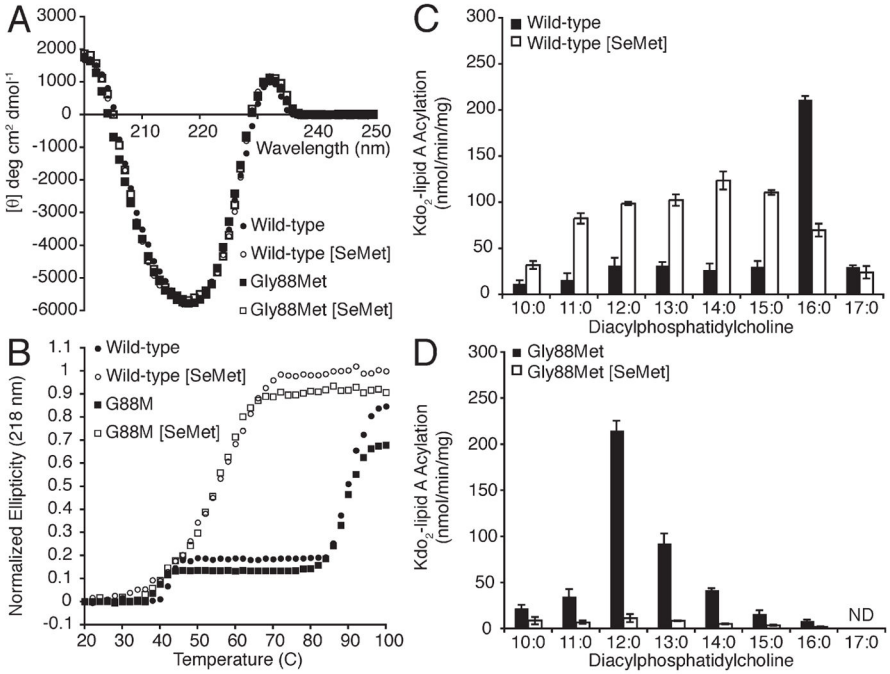

Figure 6.

SeM substitution is highly destabilizing to PagP.Far-UVCD(A) and thermal melts at 218 nm(B) reveal that substituting methionines in wild-type and Gly88Met PagP with SeM compromises stability. PagP specific activity was measured using defined PtdCho's varying in saturated acyl chain length from C17 to C10. Wild-type (C) and Gly88Met (D) PagP were monitored with and without SeM substitution. ND means not detected.

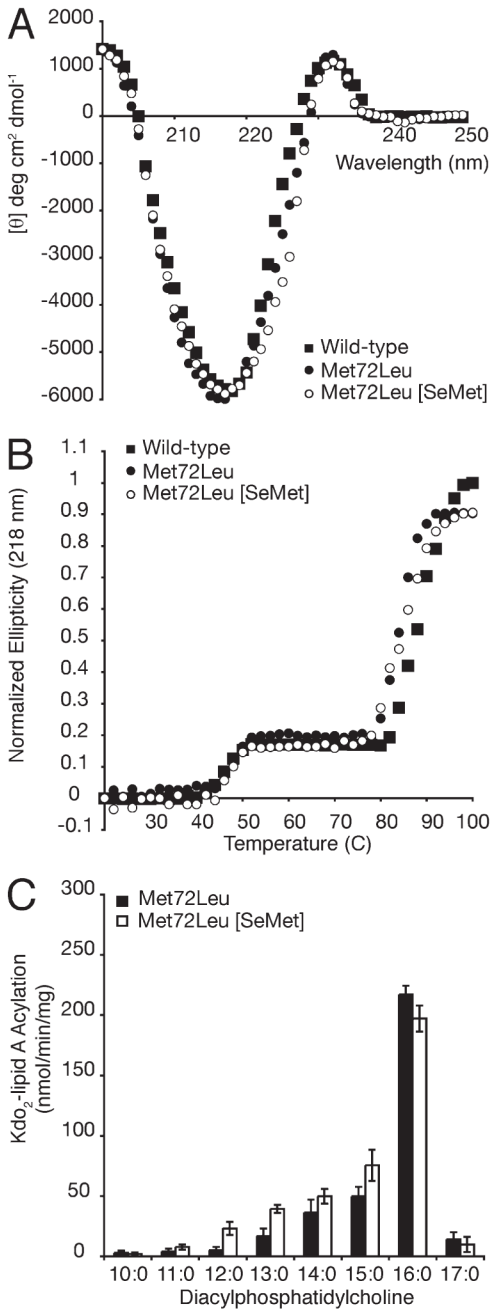

Figure 7.

SeM destabilization is attributed to Met72. Far-UV CD (A) and thermal melts at 218 nm (B) reveal that substituting methionines in Met72Leu PagP with SeM no longer compromises stability. PagP specific activity was measured using defined PtdCho's varying in saturated acyl chain length from C17 to C10. (C) Met72Leu PagP was monitored with and without SeM substitution.

Table 1

Electrospray Ionization Mass Spectrometry of Modified PagP Mutants

	exact mass (Da)	experimental mass (Da)
wild type[a]	20175.49	20174.53±0.4
Gly88Met[a]	20249.64	20249.41±0.7
Gly88Cys[a]	20221.58	20220.15±0.6
[*S*–*S* dimer]	[40441.14]	[40439.32±1.0]
G88C-*S*-methyl[a]	20235.61	20234.53±0.5
G88C-*S*-ethyl	20249.64	20251.10±1.9
G88C-*S*-*n*-propyl	20263.67	20263.50±1.4
G88C-*S*-*n*-butyl	20277.77	20277.20±1.9
G88C-*S*-*n*-pentyl	20291.73	20291.78±1.8
G88C-*S*-*n*-hexyl	20305.76	20305.71±1.8
G88C-*S*-*n*-aminopentyl	20308.77	20309.51±1.9
wild type [Nle]	20085.34	20084.31±2.4
Gly88Met [Nle]	20141.46	20141.71±1.9
Gly88Cys [Nle]	20131.43	20129.81±1.0
[*S*–*S* dimer] [Nle]	[40260.84]	[40258.63±2.4]
G88C-*S*-ethyl [Nle]	20159.49	20159.01±1.9
Met72Leu	20157.46	20155.40±3.5
Met72Leu [SeM]	20345.04	20344.01±3.6
wild type [SeM]	20409.99	20409.35±1.9
Gly88Met [SeM]	20531.04	20529.31±2.2

[a]The wild-type *E. coli* PagP protein used in this study lacks the N-terminal signal peptide and contains a C-terminal His_6 tag. The amino acid sequence with Gly88 underlined and the five methionine residues in italics: *M*NADEW*M*TTFRENIAQTWQQPEHYDLYIAITWHARFAYDKEKTDRYNERPWGGGFGLSRWDEKGNWHGLYA*M*AFKDSWNKWEPIAG YG̲WESTWRPLADENFHLGLGFTAGVTARDNWNYIPLPV LPLASVGYGPVTFQ*M*TYIPGTYNNGNVYFAW*M*RFQFLEHHHHHH. A disulfide-linked dimeric species of the Gly88Cys mutant is observed by this ESI-MS procedure, which was previously developed to validate the G88C-*S*-methyl mutant (21).